

Failure Analysis and Optimization of Aircraft Wheel Hub for Optimum Landing Scenario

Ejiroghene Kelly Orhorhoro*¹, Ikpe Aniekan Essienubong^{#2}, Oyejide Oluwayomi Joel^{#3}

*¹ Department of Mechanical Engineering, College of Engineering, Igbinedion University, Okada, Nigeria

^{#2} Department of Mechanical Engineering, Coventry University, United Kingdom

^{#3} Department of Mechanical Engineering, Federal University of Petroleum Resources, Effurun, Nigeria

Abstract

Wheel hub of an aircraft serves various functions; it allows the aircraft for safely and successfully landing and it equally support aircraft at rest condition. In the past, series of failure had been reported with aircraft as a result of damage to the aircraft wheel hub. This study focuses on the failure analysis and optimization of aircraft wheel hub for optimum landing scenario. LS-DYNA software was used for the analysis. To run the initial static analysis of the hub, the hub model was constrained at the centre. The impact forces act on the wheel from the point of impact and are expected to travel through the entire elements of the tyre. In the first model, 8022N was applied and this was divided among 135 nodes. The nodes are selected to receive direct impact load from the hub. The forces act in the positive y-direction. While for the second model, 4011N is applied and it is divided among 270 nodes. The nodes are selected to be a little closer to the semi line of the hub. Aluminium alloy A356.2 and aluminium alloy 5086-H32 were used for both the initial and final analysis of the aircraft wheel hub. Reduced weight and stresses was achieved by replacing aluminium alloy A356.2 with aluminium alloy 5086-H32 which had a lower mass density (kg/m^3), higher tensile strength (MPa) and slightly higher elastic modulus (MPa). The increased in modulus of elasticity helped to increase the rate at which the wheel hub would resist deformation in response to the upward and downward forces acting on the wheel during landing of the aircraft.

Keywords — Failure analysis, aircraft; landing scenario, wheel hub; optimization, LS-DYNA software

I. INTRODUCTION

Aircraft wheel hub plays a vital role in the landing scenario of an aircraft. It is critical for aircraft safety and performance upon landing and taxiing on the ground. The compatibility between the wheel hub and the rest components is an important requirement for safe landing, thus, certification [1]. Wheel hub of an aircraft serves various functions; it allows an aircraft for safely and successfully landing and it equally support aircraft at rest condition [2].

Generally, all aircraft components are monitored and maintained through continuous inspection using a testing method which must meet the international standard. The routine inspection of main components such as the aircraft wheel hub is performed based on the lifetime and priority scale according to the international flight regulations [3]. Inspections are usually carried out on the wheel hub to ensure that; the wheel tie bolts are secure and have not worked loose. Also to check corrosion, cracks, or other visible damage, inspection of brake disc for evidence of cracks, deep grooves, excessive wear, or other visible damage. However, several engineering factors such as impact load, vibration and weight of the airplane affect the aircraft wheel. Under varying load, the wheel hub is subjected to fatigue. Fatigue fracture is a continuous cyclic stress on the material, which occurs as a result of crack initiation and crack nucleation in the material [5-6]. Some aircraft components such as wheel hub failed due to the existence of cracks. The kinds of crack found in the wheel hub are usually fatigue cracks [6]. The crack formation is due to factors such as surface roughness of run way. The rough surface of run way can increase load fluctuation of all aircraft components, so that the difference between minimum and maximum loads tend to be higher [7]. The wheel hub comprised of an inboard and outboard section (Fig. 1). The fatigue crack is initiated in the stress-concentrated; transition region between the bearings bore wall and the circumferential radius (Fig. 2). The direction of crack nucleation is shown by the arrow.

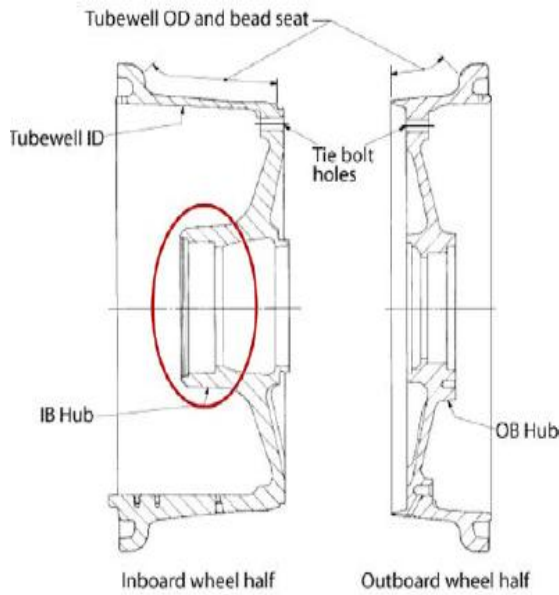


Fig 1: Wheel Hub (Failure Location Circle)



Fig 2: Fractured Hubs from the Inboard Wheel Half

In wheel hub development and design, three major wheel tests are used [8]; rotating bending test, radial fatigue test, and impact test. In spite of the fact that most engineers and designers are aware of fatigue and that a huge amount of experimental data has been generated on the fatigue properties of various metallic and non-metallic materials, fatigue failures of engineering components is still a common phenomenon [9]. Furthermore, Von Mises yield criterion which is known as a maximum distortion energy theory of failure is an important tool for failure analysis. Von Mises suggests that yielding of a ductile material begins when the second deviatoric stress invariants reaches a critical value [10]. Generally, distortion energy required per unit volume, U_d for a 3 dimensional case is given by equation (1).

$$U_d = \frac{1 + \mu}{3E} \left[\frac{(\sigma_1 - \sigma_2)^2 + (\sigma_2 - \sigma_3)^2 + (\sigma_3 - \sigma_1)^2}{2} \right] \quad (1)$$

Nevertheless, distortion energy for simple tension case at the time of failure is given by equation (2):

$$U_d = \frac{1 + \mu}{3E} \sigma_y^2 \quad (2)$$

Combining equation (1) and equation (2);

$$\sqrt{\left[\frac{(\sigma_1 - \sigma_2)^2 + (\sigma_2 - \sigma_3)^2 + (\sigma_3 - \sigma_1)^2}{2} \right]} \geq \sigma_y \quad (3)$$

Von Mises stress is given by the left side of the equation.

$$\sqrt{\left[\frac{(\sigma_1 - \sigma_2)^2 + (\sigma_2 - \sigma_3)^2 + (\sigma_3 - \sigma_1)^2}{2} \right]} = \sigma_y \quad (4)$$

The failure condition is given by equation (5)

$$\sigma_y = \sigma_y \quad (5)$$

The two-pieces of aircraft wheel hub is cast or forged from aluminum (Al) or magnesium (Mg) alloy. The halves are attached together and contain a groove at the coupling surface for an O-ring, which seals the rim since most modern aircraft utilize tubeless tires [11-12]. The bead seat area of the wheel which is the exact place where the tire actually contacts the wheel is a critical area that accepts the significant tensile loads from the tire during landing [13-15]. However, to strengthen and improved this area during design and manufacturing stage, the bead seat area is typically rolled to pre stress it with a compressive stress load. The main parts comprise of the inner and outer wheel hubs, tie bolts, heat shields, O ring, over inflation valve, thermal relief valves, and disk alignment brackets [16-17]. Aircraft wheel hub composed of numerous actuation mechanisms and structural bracing components interconnected together. Their main function is to enable movement while on the ground, and improve aerodynamic efficiency by being stowed away during flight and stability during landing scenario. However, wheel hub failure had been a common occurrence in the aviation industry. Due to weight and space limitations, few redundancy features exist within landing wheel hub. Thus, wheel hub must endure the extreme impact and vibrational loading experienced during landing and braking, and are consequently deemed critical components [18-19]. Considering the sensitive nature of aircraft and the effect and casualties that might results in case of failure, it became necessary to carry out failure analysis and optimization of wheel hub of aircraft

II. RESEARCH METHODOLOGY

A. Design Specification

To achieve optimum results, the following design specifications were used for both the initial and final analysis of the aircraft wheel hub.

- 1) Probe: absolute point probe, 5 mm to 10 mm in diameter, frequency; 100 KHz ~ 2 MHz

- 2) Wheel hub outer diameter range: 0 ~ 800 mm
- 3) Wheel hub inter diameter range: 70 ~ 200 mm
- 4) Distance of travel for lifter: 210mm
- 5) The speed for probe movement: probe X/Y moving speed up to 200 mm/s
- 6) Wheel hub operation: rolling platform, with height and angle position encoder, safety elevate and inertia aligning
- 7) Surface detection speed: the largest is 2 m/s
- 8) Spiral scan step pitch: 0 ~ 25 mm, adjusting unit 0.1 mm
- 9) Overall dimension: 1050 * 1050 * 1050 (mm)

B. Material Properties

The material properties for the initial analysis are presented in Table 1.

Table 1: Initial Material Property

Material Properties	Aluminium Alloy A356.2
Young's Modulus	69000 MPa
Poison's Ratio	0.33
Mass Density	2.685e-006 kg/mm ³
Thermal Expansion	1.2e-005/°C
Yield Strength	250 MPa
Ultimate Tensile Strength	279 MPa

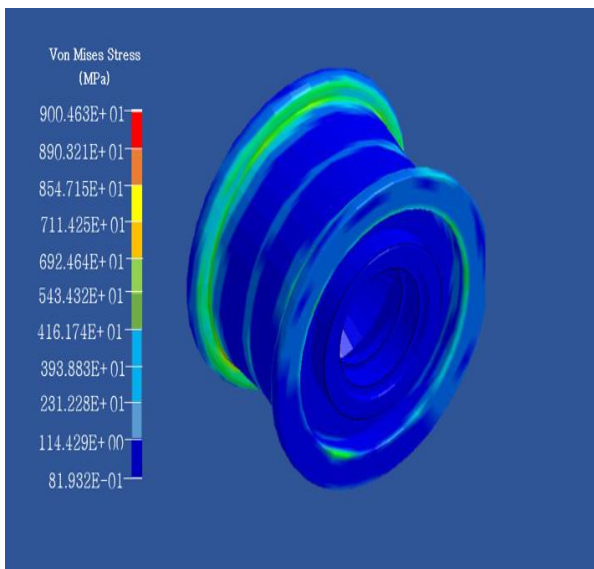


Fig 3: First Analysis with First Load case of 8022N

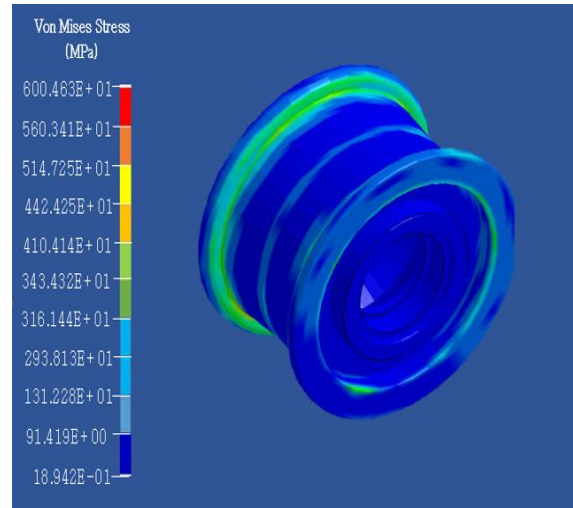


Fig 4: Second Analysis with Second Load case of 4011N

At the end of the first analysis, maximum weight for the wheel hub was 250 kg. Similar analysis was carried out on the will hub with few changes to the material and properties to observe the differences.

Table 2: Final Material Property

Material Properties	Aluminium Alloy 5086-H32
Young's Modulus	70999 MPa
Poison's Ratio	0.33
Mass Density	2.660e-006 kg/mm ³
Thermal Expansion	2.4e-005/K
Yield Strength	193 MPa
Ultimate Tensile Strength	290 MPa

C. Hub Mesh

The mesh for the hub was already available in the LS-DYNA keyword format. To import the Hub mesh, the LS-DYNA solver is selected at the prompt for HYPER MESH as displayed in Fig. 5. The import solver deck command is shown in Fig. 6 which was used to import the keyword file of the Hub mesh directly into HYPERMESH. Fig. 7 shows the imported mesh of the tyre Hub.

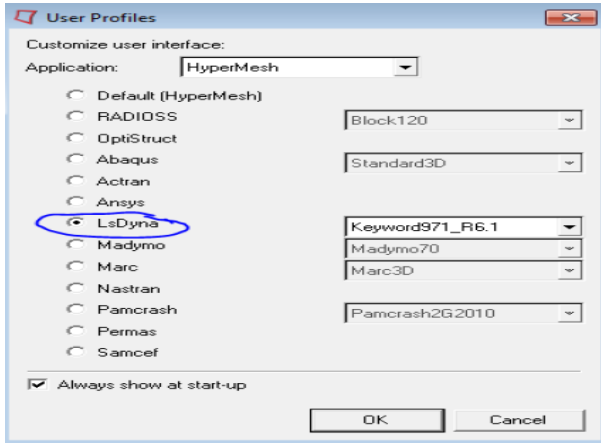


Fig 5: LS-DYNA Solver Selector

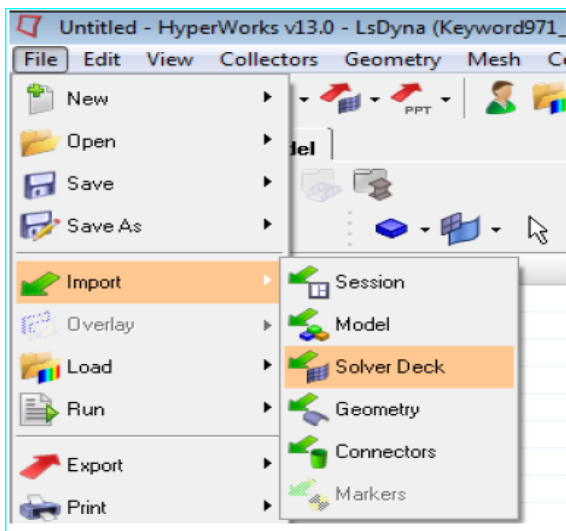


Fig 6: Solver Deck Import for Keyword File

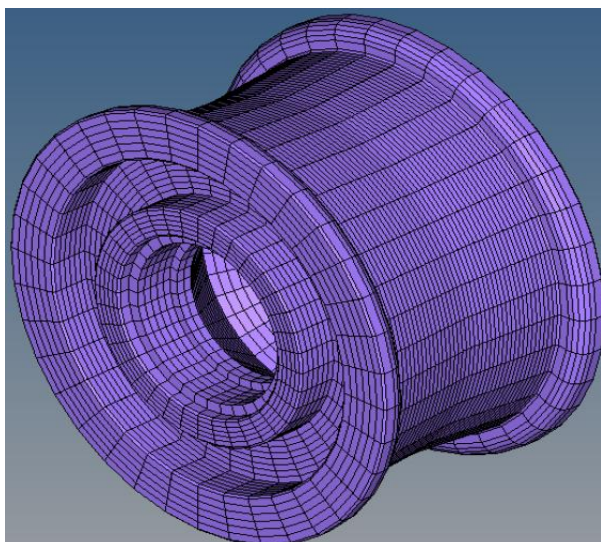


Fig 7: Imported Hub Mesh

D. Loads and Boundary Conditions

To run the initial static analysis of the hub, the hub model was constrained at the centre presented in Fig. 8. The impact forces act on the wheel from the point of impact and are expected to travel through the entire elements of the tyre. The only challenge with the hub design is that the hub must be symmetric as the cross-section at all points in the wheel must be the same. This is so because any side of the wheel could be involved in the impact at any particular point. The loads on the tyre are expected to be tested to select a more suitable one. The first model of the force applies exactly the same amount of force divided among 135 nodes. The forces on each node are 8022N. The nodes are selected to receive direct impact load from the hub. The forces act in the positive y-direction. The second model of the force applies exactly the same amount of force like the first model divided among 270 nodes. The force on each node is 4011N. The nodes are selected to be a little closer to the semi line of the hub. The first and the second force model are shown in Fig. 9 and Fig. 10 respectively.

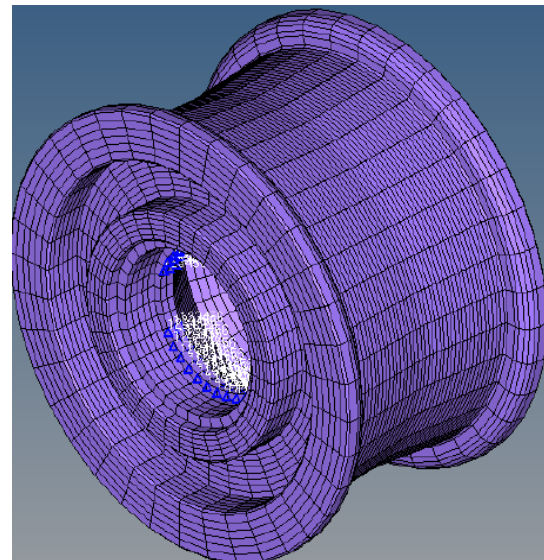


Fig 8: Hub Mesh with SPC

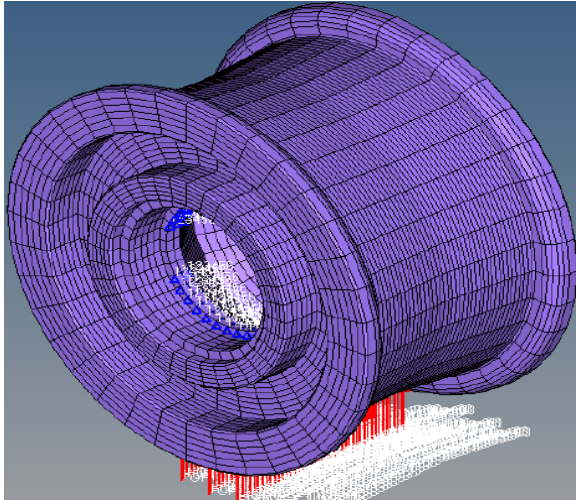


Fig 9: Hub with First Load Distribution

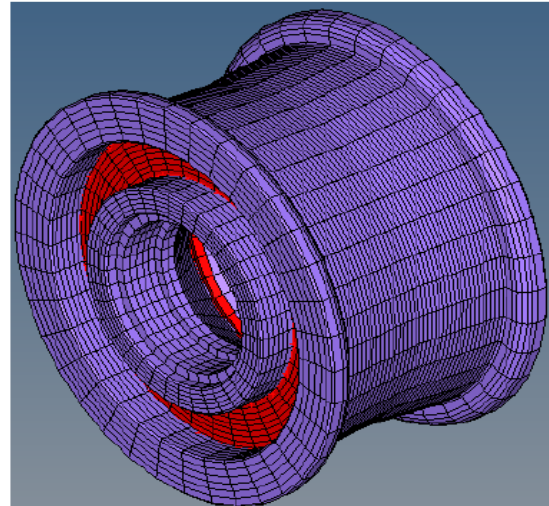


Fig 11: Hub Mesh Divided into Two Regions

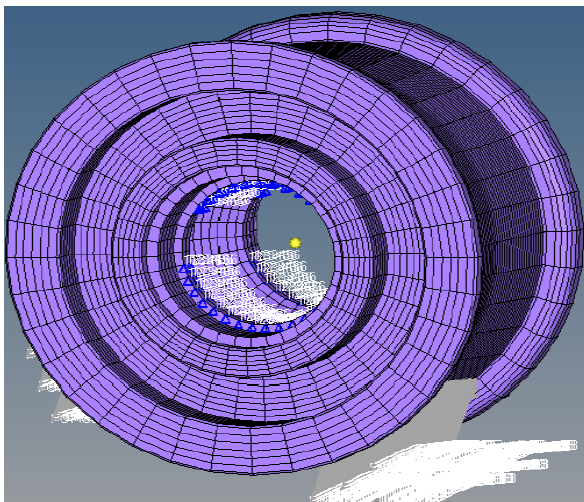


Fig 10: Hub with Second Load Distribution

E. Optimization Design Space

To optimize the hub, the mesh of the hub was divided into two parts (Fig. 11). The region coloured red in the figure is prepared as the design space. The optimization model was prepared in such a way that it can remove material from the entire model.

III.RESULTS AND DISCUSSION

Static analysis of the hub was carried out using the two load cases described. For the first load case, the stress on the hub is maximum at 94.4MPa. The contour plot of the stress from the first load case is shown in Fig. 12.

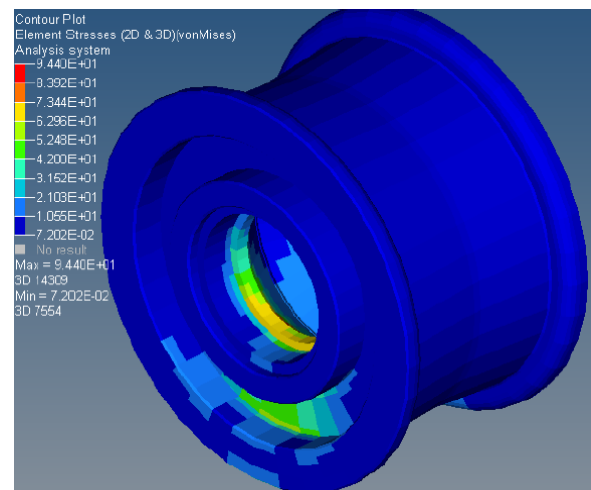


Fig 12: Stress Plot on the Hub for First Load Case

For the first load case, the maximum displacement in the hub from the static analysis in HYPERMESH is 0.1mm. The contour plot of the displacement of the hub for the first load case is shown in Fig. 13.

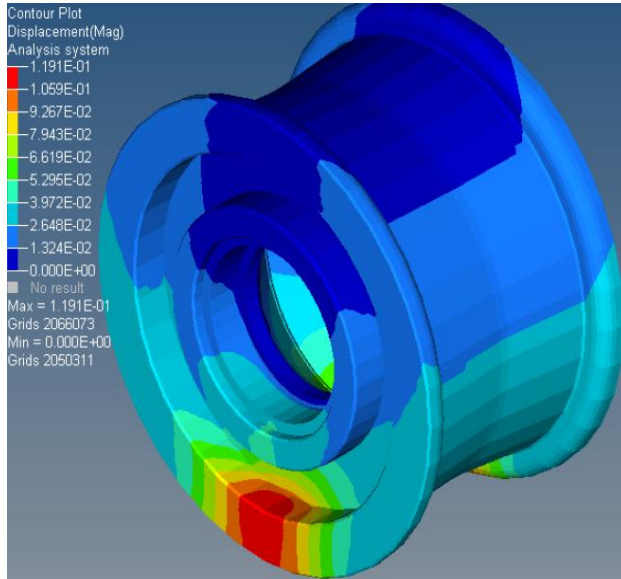


Fig 13: Displacement plot on the Hub for First Load Case

For the second load case, the stress on the hub is a maximum at 57.1MPa. The contour plot of the stress from the second load case is shown in Fig. 14.

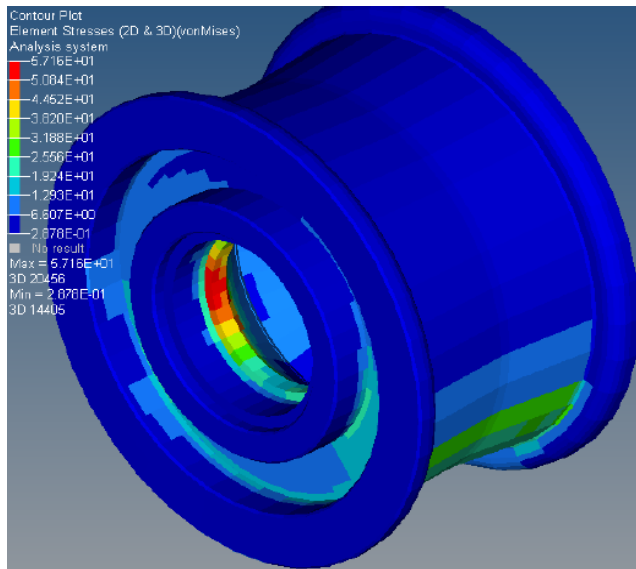


Fig 14: Stress Plot on the Hub for Second Load Case

For the second load case also, the maximum displacement in the hub from the static analysis in HYPERMESH is 0.0744mm. The contour plot of the displacement of the hub for the second load case is shown in Fig. 15.

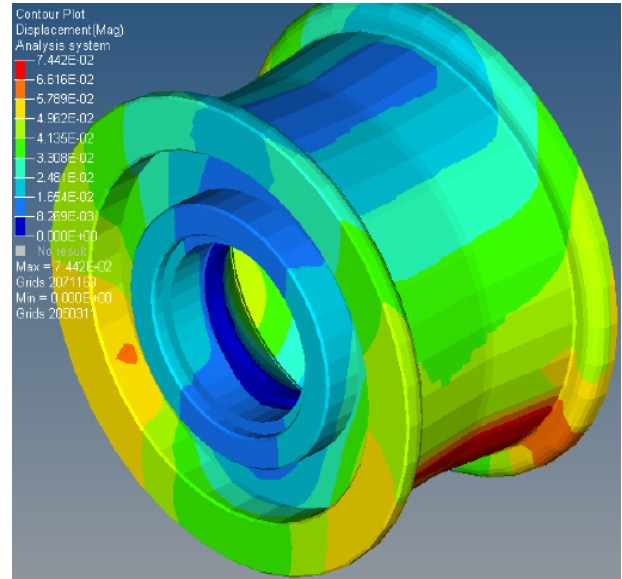


Fig 15: Displacement plot on the Hub for Second Load Case

After the initial analysis, maximum weight for the wheel hub was obtained as 250 kg. However, this weight reduced to 187 kg as a result of design optimization of the wheel hub. Reduced weight and stresses were achieved by replacing aluminum alloy A356.2 with aluminum alloy 5086-H32 which had a lower mass density (kg/m^3), higher tensile strength (MPa) and slightly higher elastic modulus (MPa). Similar analysis was carried out on the wheel hub with few changes to the material properties to observe the differences. The results of the analysis shown that Von Mises stress of 94.4MPa was acting on wheel hub produced from Aluminium alloy A356.2 and this gave a safety factor of 2.648. However, for the wheel hub produced from aluminium alloy 5086-H32, Von Mises stress of 57.1MPa acted on it and this gave a safety of factor of 3.380. In both cases, the Von Mises stresses are less than yield stresses, thus the wheel hub will hardly fail from the induced stresses. However, the safety of the wheel hub was improved by replacing aluminium alloy A356.2 with aluminium alloy 5086-H32. This resulted in an increased in modulus of elasticity and consequently increase the rate at which the wheel hub would resist deformation in response to the upward and downward forces acting on the wheel during landing of the aircraft. Besides, the lower mass density of the new material would improve fuel efficiency and as well safe cost.

IV. CONCLUSIONS

The research work presented successfully demonstrated failure analysis and optimization of aircraft wheel hub for optimum landing scenario. Static analysis of the hub was carried out using two loading cases with two different aluminum alloys.

For the first load case, the stress on the hub was maximum at 94.4MPa while the maximum displacement in the hub from the static analysis in HYPERMESH was 0.1mm. For the second load case, the maximum displacement in the hub from the static analysis in HYPERMESH was 0.0744mm while the stress on the hub was maximum at 57.1MPa. Since the Von Mises stresses in both cases are less than the yield stress, the wheel hub fabricated from both aluminum alloys will not fail at the induced stress. However, for optimization, improved safety factor, increased in modulus of elasticity, and resistant to deformation resulting from upward and downward forces acting on the wheel during landing of the aircraft, aluminium alloy 5086-H32 is preferable.

REFERENCES

- [1] A. Teo, K. Rajashekara, J. Hill, and B. Simmers, Examination of Aircraft Electric Wheel Drive Taxiing Concept, SAE International, pp. 2008-01-2860, 2008
- [2] G. Kuldip, and D. Vishal, Design optimization of landing gear of an aircraft- a review, Journal of Mechanical and Civil Engineering (IOSR-JMCE), pp. 01-04, 2014
- [3] M.N. Ilman, Failure Analysis of a Wheel Hub Made From 2014-T61 Aluminium Alloy, Research Report, Laboratorium Bahan Teknik, Jurusan Teknik Mesin UGM, Yogyakarta, 2003
- [4] W. Song, L. Woods, T. Davis, T. Offutt, P. Bellis, S. Handler, K. Sullivan, and W. Stone, Failure analysis and simulation evaluation of an AL 6061 alloy wheel hub, Journal of Failure Analysis and Prevention, 15(4), pp. 521-533, 2015
- [5] S.K. Johnshaw, L. Gangadhar, and K.T. Sunil, Finite element fatigue analysis of mg alloy (am60) aircraft wheel hub, International Journal of Engineering Sciences and Research Technology, 5(11), pp. 549-554, 2016
- [6] P.L. Minh, Fatigue limit evaluation of metals using an infrared thermography technique, Mechanics of Materials., 28(4), pp. 155-163, 1998
- [7] H.H. Jamasri, Failure analysis of wheel hub made from Al 2014-T61, Jurnal Teknik Gelagar, 16(02), pp. 102 – 109, 2005
- [8] Y.L. Hsu, S.G. Wang, and T.C. Liu, Prediction of fatigue failure of aluminum disc wheel using the failure probability contour based on historical test data, Journal of China Institute of Industrial Engineering, 21(6), pp.551–558, 2014
- [9] P.R. Raju, B. Satyanarayana, K. Ramji, and K.S. Babu, Evaluation of fatigue life of aluminum alloy wheels under bending loads, Fatigue & Fracture of Engineering Materials and Structures, 32(2), pp. 119-126, 2009
- [10] R.M.A. Christensen, A comprehensive theory of yielding and failure for isotropic material, Journal of Engineering Material Technology, 129, pp. 173-181, 2007
- [11] M.M. Topac, S. Ercan, and N.S. Kuralay, Fatigue life prediction of a heavy vehicle steel wheel under radial loads by using finite element analysis, Engineering Failure Analysis, 20(3), pp. 67-79, 2012
- [12] H. Guo, An investigation into the finite element modeling of an aircraft tyre and wheel assembly. Unpublished PhD Thesis. Coventry: Coventry, 2014
- [13] K.J. Josin, Analysis of Aircraft Wheel Hub Assembly Using NDT Techniques, International Advanced Research Journal in Science, Engineering and Technology, 3(5), pp. 17-20, 2016
- [14] B. Kosec, G. Kovacic, L. Kosec, Fatigue crack of an aircraft wheel,” Engineering Failure Analysis, 9, pp. 603-609, 2008
- [15] X. Yang, Generation of Tyre Cross-Sectional Geometry for FE Tyre Model using Image Processing Techniques, International Journal of Engineering Simulation, 10(1), pp.3-10, 2009
- [16] N.A. Siddiqui, K.M. Subair, M. Azhar, K.M. Deen, and M.A. Amin, Failure investigation of wheel gear hub assembly of an aircraft, Engineering Failure Analysis, 22, pp. 73-82, 2012
- [17] H. Guo, C. Bastien, M. Blundell, G. Wood, Development of a Detailed Aircraft Tyre Finite Element Model for Safety Assessment, Journal of Materials & Design, 53, pp. 902-909, 2014
- [18] P. Wang, L. Dacko, Aircraft Level Steering Runaway Failure Analysis,” SAE International, 2009-01-3136
- [19] M. Behroozi, O.A. Olatunbosun, W. Ding, Finite Element Analysis of Aircraft Tyre – Effect of Model Complexity on Tyre Performance Characteristics, Journal of Materials and Design, 25, pp. 810-9, 2012